

# The hot compaction of high modulus melt-spun polyethylene fibres

P. J. HINE, I. M. WARD

*Interdisciplinary Research Centre in Polymer Science and Technology, University of Leeds, Leeds LS2 9JT, UK*

R. H. OLLEY, D. C. BASSETT

*J.J. Thompson Physical Laboratory, University of Reading, P.O. Box 220, Whiteknights, Reading RG6 2AF, UK*

The production of solid section highly oriented polyethylene by compaction of melt-spun polyethylene fibres is described. Differential scanning calorimetry, X-ray diffraction and electron microscopy have been used to determine the structure of the compacted polymer. The essential feature of the process is shown to be selective surface melting of the fibres to form a polyethylene/polyethylene composite of very high integrity, yet maintaining a very high proportion of the strength and stiffness of the fibres.

## 1. Introduction

The last 20 years have seen the development of high-stiffness and high-strength polymers by a number of different processing routes [1, 2]. For polyethylene, a major development has been the manufacture of high-stiffness fibres, by drawing isotropic fibres to a very high draw ratio. The isotropic fibre can be made either by melt spinning of low molecular-weight polymer [3], or by gel-spinning high molecular-weight polymer [4]. Values of fibre modulus obtained are in the range 40–100 GPa.

A further development has been the production of oriented polymer rods, sheets and tubes by hydrostatic extrusion or die-drawing, where large-section products are made by forcing the isotropic polymer through appropriate dies by the application of hydrostatic pressure or tensile drawing. Although both hydrostatic extrusion and die drawing can produce materials of high stiffness and strength, this is often at the expense of production speed, so that in practice reduced enhancement of properties may have to be accepted (maximum modulus < 30 GPa).

There is therefore a considerable incentive to explore the possibilities that high stiffness can be achieved in large section by incorporation of very high-modulus fibres. In this paper we examine the potential of hot compaction to make large-section products from high-modulus polyethylene fibres. The compacted materials also offer an alternative route to producing polyethylene/polyethylene composites, an area of current research interest (e.g. [5]). By manufacturing such composites using only one phase, any problems with the dispersion of a second phase are avoided, which has obvious benefits in ease and cost of processing.

This paper describes a manufacturing route for successful compaction of melt-spun polyethylene fi-

bres. The elements that control the compaction process, notably temperature, time and pressure, have been investigated. Samples have been produced using different processing conditions and then assessed in terms of their stiffness, strength and density. Differential scanning calorimetry and X-ray diffraction have been used to study the mechanisms of the compaction process. Finally, the internal microstructure of the compacted materials has been examined using sectioning and etching techniques.

## 2. Experimental procedure

Initial experiments showed that the three important process variables were the compaction temperature, the compaction pressure and the time of compaction. It was quickly established that the most critical of these was the compaction temperature. The majority of the work has therefore concentrated on studying the effect of varying the compaction temperature while keeping all other conditions fixed. A typical compaction procedure would follow the following route.

The fibres are first arranged unidirectionally in a matched metal mould and then placed into a heated compression press which is maintained at the compaction temperature. Contact pressure of 0.7 MPa (100 p.s.i.) is applied and the mould is allowed to soak for 10 min. Finally, a pressure of 21 MPa (3000 p.s.i.) is applied for 10 s before removing the mould from the press and allowing it to cool slowly. All the parameters in italics are process variables which in some way affect the final properties of the compacted material.

The fibre used in all the tests was a melt-spun high-modulus polyethylene fibre manufactured commercially by Snia Fibre, Italy, with the trade name Tenfor. The fibre was in the form of a multifilament yarn of filaments, each of nominal diameter 10 µm giving a

yarn denier of  $217 \text{ g km}^{-1}$  (the weight in grams of 9000 m of fibre). The molecular weight characteristics of the polymer were a number-average molecular weight of 17 000 and a weight-average molecular weight of 150 000.

Evaluation of the properties of the compacted materials used a number of different techniques. The strength and stiffness of the compacted materials were measured under three-point bend conditions following ASTM 790 [6], using a servo-mechanical tensile testing machine (RDP Howden Ltd). The densities of the compacted materials were measured using either a density column or a density bottle. The density column used a mixture of isopropanol and diethylene glycol at a temperature of  $23^\circ\text{C}$ . The melting behaviour of the compacted materials was investigated using a Perkin-Elmer DSC7 differential scanning calorimeter. A scanning rate of  $10^\circ\text{C min}^{-1}$  was used for all the tests. The orientation of the virgin fibre and the compacted materials was measured using a Siemens X-ray diffractometer.

The microstructure within blocks of fibres compacted at  $138^\circ\text{C}$  was examined with the transmission electron microscope. For this purpose, the material was cut, with a microtome and diamond knife, either along or transverse to, the average fibre direction. The exposed surfaces were etched with a permanganic reagent [7-9], then replicated by a standard two-stage technique. Full details are given in the following paper [10]. The illustrations displayed in this paper are all of shadowed, carbon replicas of these etched surfaces.

### 3. Results

The very first compaction experiments were performed at room temperature but it became clear that the transverse strengths of these materials, even for very high compaction pressures and long compaction times, were poor. Although increasing the compaction temperature to  $100^\circ\text{C}$  showed an improvement in the transverse strength with no loss of fibre modulus, the materials produced were still relatively weak and were white and opaque in appearance. With further increase of the compaction temperature to temperatures within the melting range of the fibre, the compacted material showed a transition from white to translucent in colour. Remarkably, it appeared from DSC studies that these materials still retained a significant proportion of the virgin fibre phase.

In our initial experiments, very long compaction times were used, sometimes as long as 2 h. However, once the optimum temperature range was discovered, it was soon found that reducing the compaction time (the time under high pressure) did not affect the compacted material properties. Furthermore, it was shown that the time under high pressure need only be very short for successful compaction. A value of 10 s was therefore adopted for all subsequent experiments.

The role of the initial low-pressure stage of the compaction process appears to be merely to hold the fibres together while changes occur which are determined by the compaction temperature. Applying high

pressure during this initial phase resulted in a poor compaction product.

The following experiments investigate the critical nature of the compaction temperature while maintaining all other parameters fixed at the values shown in Section 2.

#### 3.1. DSC measurements

The transition in compacted material behaviour, around the onset of melting, was first examined using differential scanning calorimetry. The onset of melting for the fibre is defined in this paper as the intercept on the abscissa of the extrapolated leading edge of the DSC melting endotherm. Fig. 1 shows a DSC run on material compacted at  $138^\circ\text{C}$ , compared with a similar run on the virgin fibre. The important difference in melting behaviour is the appearance of a lower melting point peak in the compacted material. An immediate inference is that during compaction at  $138^\circ\text{C}$  a small amount of the original fibre was melted which, on cooling, reformed in a different textural form with a lower melting point.

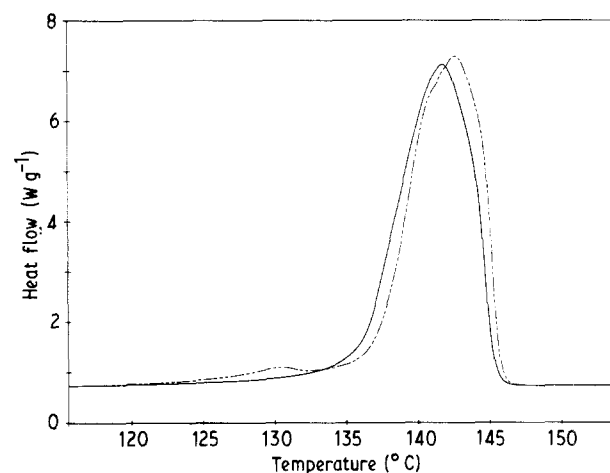


Figure 1 DSC melting endotherm (normalized) of a sample compacted at  $138^\circ\text{C}$  (---). (—) original fibre.

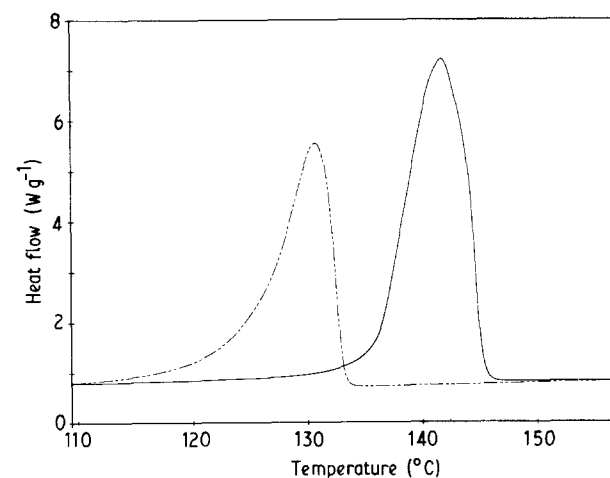


Figure 2 DSC melting endotherm (normalized) of the original fibre (—) and the same fibre after cooling and subsequent reheating (---).

To confirm this idea, a simple experiment was performed. A sample of the virgin fibre was heated in the calorimeter to above its melting point using a scanning rate of  $10^{\circ}\text{C min}^{-1}$ , cooled at  $100^{\circ}\text{C min}^{-1}$  to  $20^{\circ}\text{C}$  and then rescanned at  $10^{\circ}\text{C min}^{-1}$ . The results of these two runs are shown in Fig. 2. The position of the melting peak has shifted from  $141^{\circ}\text{C}$  for the first run, to  $130^{\circ}\text{C}$  for the second run. The position of the melting peak for the second run correlates exactly with the position of the smaller peak in Fig. 1. This is consistent with the view that the two separate melting peaks do not arise from fractionation of the polymer, i.e. two species of different molecular weights. Comparison with the literature (e.g. [11]) identifies the lower melting point material as isotropic polyethylene.

Clearly the consequence of complete melting is the destruction of the microstructure associated with the virgin fibre and recrystallization into another form. A compaction temperature within the melting range will melt only part of the sample, with the remainder influencing subsequent crystallization.

The next key issue was to investigate the effect of varying the compaction temperature, because by accurately controlling the temperature it should be possible to control the proportions of the original and modified components. Samples were therefore made at a range of compaction temperatures from  $134$ – $142^{\circ}\text{C}$  and then examined using the DSC, with the following results.

Samples compacted at  $134^{\circ}\text{C}$  showed no evidence of any second component: this is not unexpected as this temperature is outside the melting range of the fibre. Samples compacted at  $136^{\circ}\text{C}$  showed only a tiny amount of melted and recrystallized material. Fig. 3 shows the melting endotherms for three further compaction temperatures,  $138$ ,  $140$  and  $142^{\circ}\text{C}$ , in comparison with the melting behaviour of the virgin fibre. Samples compacted at  $138^{\circ}\text{C}$ , as seen previously in Fig. 1, showed a clear low-melting peak. As the compaction temperature was further increased, the size of the lower melting peak increased at the expense

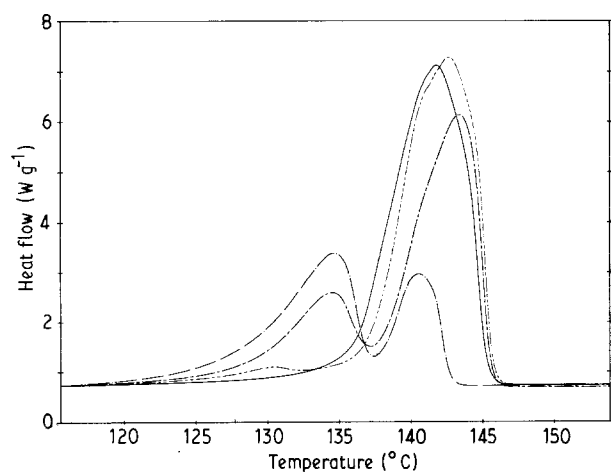


Figure 3 DSC melting endotherm (normalized) for samples compacted at (— — —)  $138^{\circ}\text{C}$ , (— · —)  $140^{\circ}\text{C}$  and (· · ·)  $142^{\circ}\text{C}$ . (—) original fibre.

of the original peak. Clearly the choice of compaction temperature allows the proportions of the two components to be controlled between 100% of the original fibre and 100% melted and recrystallized.

Two other features of Fig. 3 are worth noting. Firstly the onset temperature of the upper peak steadily increased with increasing compaction temperature. The increase in the onset temperature indicates, as expected, that the lower melting point material is being destroyed first.

A second observation from Fig. 3 is that up to a compaction temperature of  $140^{\circ}\text{C}$  the total area of the two peaks, which is a measure of the total sample crystallinity, remains roughly similar to that of the original material even though melting has occurred. At  $142^{\circ}\text{C}$ , however, there is a significant drop in the total peak area suggesting an overall drop in the sample crystallinity. This was later confirmed by the density and X-ray measurements to be reported below.

As the two morphological components have different crystalline fractions it is not possible to use the ratios of the peak areas directly to estimate their proportions. However, by looking at the reduction in the area of the original peak, the amount of material lost through melting can be determined. Fig. 4 shows the percentage drop in the normalized area of the upper peak determined from an average of five samples from each compacted material. Over the measured temperature range the amount of original fibre is seen to decrease from 92% at  $138^{\circ}\text{C}$  to 25% at  $142^{\circ}\text{C}$ .

The most interesting fact is that successful compaction is achieved using a compaction temperature of  $138^{\circ}\text{C}$  when only 8% of the virgin fibre has been melted. This figure is close to that of the fraction of material needed to fill the gaps in a close-packed hexagonal arrangement of cylinders, which is  $(1 - \pi/(2\sqrt{3})) = 9.3\%$  of the total volume (e.g. Hull [12], p. 61). These considerations show that only a small percentage of virgin fibre melting is required to give good compaction, i.e. for the retention of fibre properties to be high.

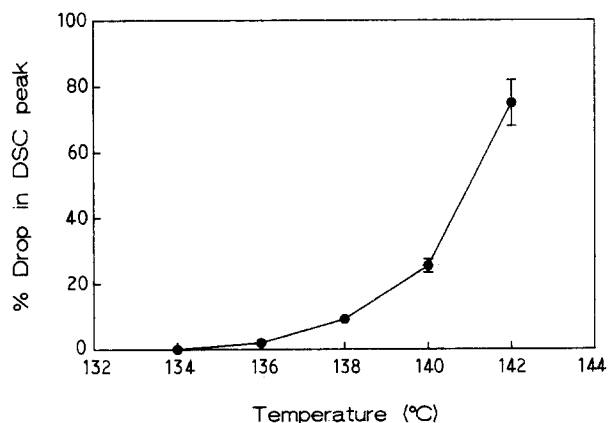


Figure 4 The percentage drop in the original fibre peak area with compaction temperature.

### 3.2. Morphological study

The use of sectioning and etching techniques allowed the internal microstructure to be investigated. At the present time this has only been attempted for samples compacted at 138 °C.

Fig. 5 shows a cross-section at right angles to the fibre direction. The sample shows perfect compaction with no evidence of any trapped air. The fibres are generally circular in shape although some sides have become faceted where two fibres meet: fibre deformation is in general limited. The fibres themselves show numerous pits on their exposed ends indicating weak channels which run down into the fibres. Close examination of the etched section shows the interstices between the fibres to be filled with a material which has a fine structure not resolvable at this magnification. Fig. 6 shows a higher magnification view of a triangular interstice created by the joining of three

fibres. The interstice is filled with lamellae of recrystallized polyethylene.

Further detail of this recrystallized material is obtained by taking a section parallel to the fibre direction. Although a longitudinal section cuts mainly down fibres, there are places where the section cuts down through the interstices. Fig. 7 shows a longitudinal section of such a region. Two interstitial regions viewed from the side now show up rather like herringbone structures. There is only weak evidence of detailed structure within the fibres themselves although there is a general impression of structure running along the fibre length.

Greater detail of an interstice is shown in Fig. 8. The recrystallized lamellae are now clearly seen to nucleate on the surface of the original fibre and then grow out away from it. Crystal growth has proceeded out from the fibres to meet in the centre leaving a clearly defined

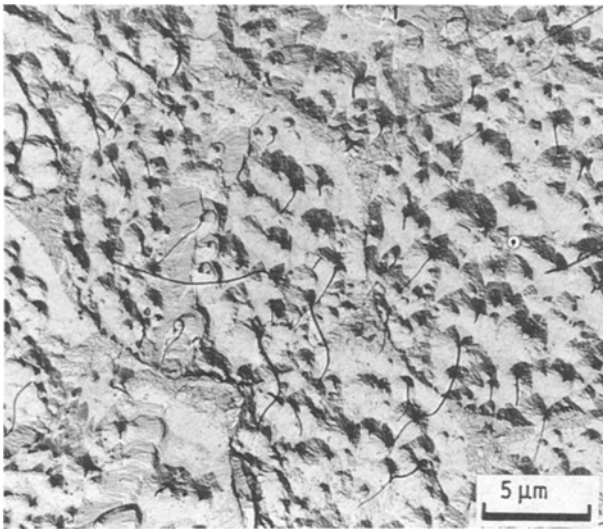


Figure 5 Etched section taken at right angles to the fibre direction. Note the pits etched within the fibres and the lamellar interfibrillar materials.

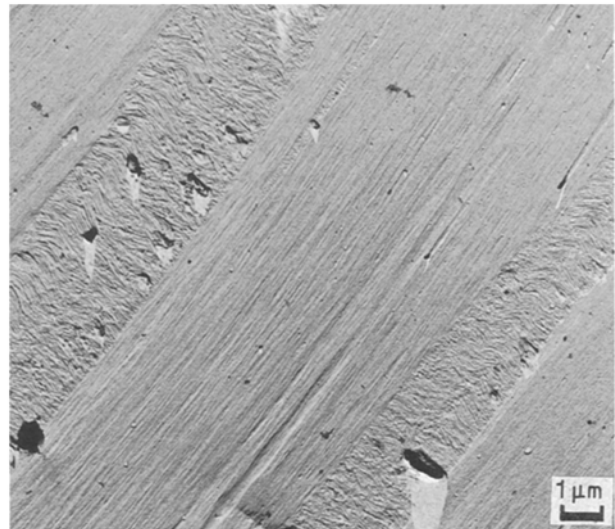


Figure 7 A longitudinal section parallel to the fibre axis, showing the fibrous and lamellar components of the texture.

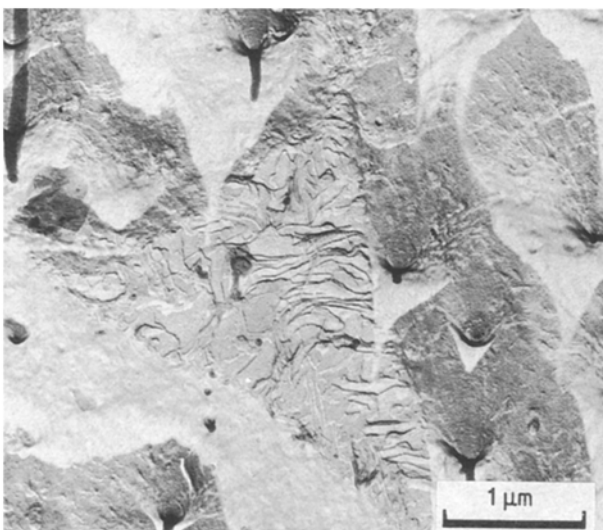


Figure 6 Close up of an interstitial region revealing lamellae which have nucleated on surrounding fibres and grown inwards.

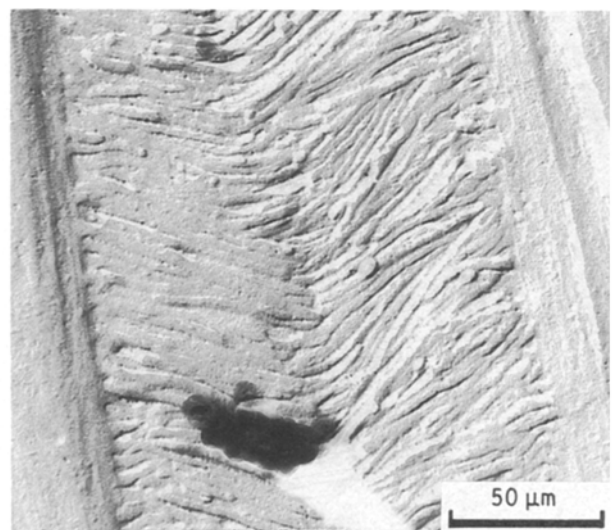


Figure 8 Detail of an interstitial lamellar region and its junction with adjacent fibres.

join. This situation is similar to that seen in plan, for example in the lower part of Fig. 8. Such structures are reminiscent of those produced in a fast-cooled metal ingot, where columnar crystals nucleate at the surface of the mould and grow out into the centre to meet [13], and of row structures in polymer crystallization [14, 15].

### 3.3. Density measurement.

The densities of the compacted materials have been measured using a density bottle for samples produced at compaction temperatures between 134 and 142 °C. Fig. 9 shows the results of these measurements in comparison with the density of the original fibre, measured to be 0.975 g cm<sup>-3</sup> using a density column.

For compaction temperatures of 134 and 136 °C, the density of the compacted material is less than that of the virgin fibre. Incomplete compaction at these temperatures, as discussed previously, will involve entrapment of air and therefore a lower density than the original fibre.

For a compaction temperature of 138 °C the relative density reaches a maximum, confirming that this is the optimum compaction temperature. The density of the compacted material does not quite reach that of the original fibre presumably because of the contribution from the recrystallized material which has a lower crystallinity than the virgin fibre. For a compaction temperature of 142 °C the much higher proportion of the recrystallized component results in a significant drop in the total crystallinity and hence a drop in the density of the compacted material.

### 3.4. Flexural modulus

The longitudinal (along the fibre direction) and transverse (perpendicular to the fibre direction) moduli were measured at room temperature in bending for samples compacted over the temperature range 134–142 °C, at a strain rate of  $7 \times 10^{-5} \text{ s}^{-1}$ .

#### 3.4.1. Longitudinal modulus

Before performing any tests on the compacted materials, the modulus of the virgin fibre was first measured.

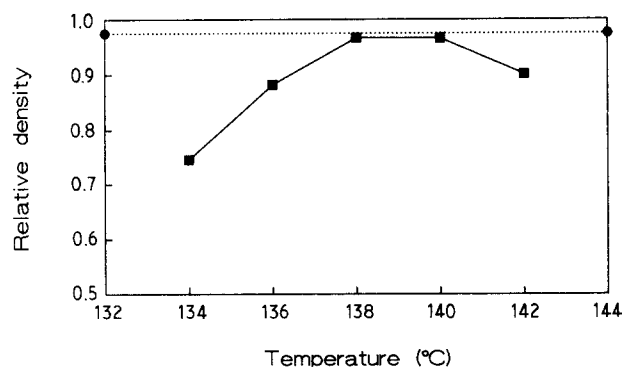


Figure 9 Compacted material relative density versus compaction temperature. (···●···) original fibre, (-■-) compacted.

The value obtained was  $42 \pm 2 \text{ GPa}$  at strain rate of  $7 \times 10^{-5} \text{ s}^{-1}$ , the same as the strain rate used for the compacted material tests. The variation of the longitudinal modulus with compaction temperature is shown in Fig. 10. At 134 °C the longitudinal modulus is much lower than the original fibre, consistent with incomplete compaction. When the compaction temperature is increased to 138 and 140 °C, and under optimum conditions, the holes in the structure are filled and the modulus rises to its maximum value. Increasing the compaction temperature above 140 °C leads to a rapid fall in longitudinal modulus, due to the substantial melting and recrystallization of the original fibre phase.

#### 3.4.2. Transverse modulus

The variation in the transverse modulus with compaction temperature is shown in Fig. 11. Unlike the longitudinal modulus, the transverse modulus does not pass through a maximum in the temperature range 138–140 °C but continues to increase with increasing compaction temperature. The transverse modulus of the original fibre will be low due to the excellent orientation of polymer chains along the fibre. The transformation of the virgin fibre phase during the compaction process will produce orientations inclined to the fibre axes and so improve the transverse modulus. For complete melting and recrystallization,

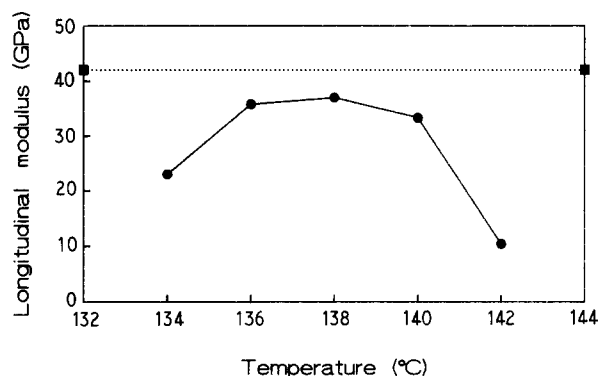


Figure 10 Longitudinal flexural modulus versus compaction temperature. (-●-) compacted, (···■···) original fibre.

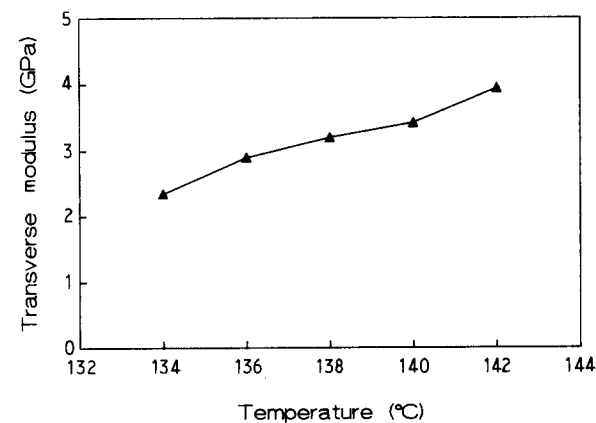


Figure 11 Transverse flexural modulus versus compaction temperature.

the two curves for longitudinal and transverse modulus should meet at the same point, i.e. the material would then be isotropic.

### 3.5. X-ray measurements

The changes in fibre orientation during compaction were studied using X-ray diffraction. As would be expected the degree of orientation of the compacted materials was worse than the virgin fibre. This could be due to two possible effects: macroscopic disorientation due to alignment problems in arranging the fibres in the compacted material, and internal changes within the fibres due to changes caused by melting and recrystallization. X-ray diffraction was used to assess the contribution from these two effects.

The sample was placed in the diffractometer with the main fibre axis in the horizontal plane. The diffractometer was fixed in  $2\theta$  space at the maximum intensity of the 002 meridional reflection (approximately  $37^\circ$ ). The sample was then rotated around its vertical axis while monitoring the X-ray intensity. This allowed the width of the 002 reflection to be determined which gave a direct measurement of the sample orientation: the narrower this peak, the better was the orientation.

Fig. 12 shows the 002 orientation peak for three samples: the virgin fibre, a sample compacted at  $136^\circ\text{C}$  and a sample compacted at  $140^\circ\text{C}$ . The degree of orientation of the sample compacted at  $136^\circ\text{C}$  decreased significantly compared to the original fibre. Interestingly, the DSC measurements showed that

little melting had occurred at this temperature so the loss of orientation must be due to macroscopic misalignment of the individual fibres. Although care was taken to ensure the fibres were well aligned, it is impossible to achieve perfect alignment and the difference in the orientation peak in Fig. 12 reflects this. The electron microscopic examinations of the following paper [10] substantiate this interpretation.

The sample compacted at  $140^\circ\text{C}$ , also shown in Fig. 12, shows a similar peak width to that compacted at  $136^\circ\text{C}$ . This proves that up to  $140^\circ\text{C}$  the orientation of the virgin fibre remains largely unchanged, and so the bulk of the fibre remains unaffected by the melting processes.

Above  $140^\circ\text{C}$ , the orientation does deteriorate. Fig. 13 shows the peak width at  $142^\circ\text{C}$  to have significantly increased compared to the sample compacted at  $140^\circ\text{C}$ . It can be concluded that above  $140^\circ\text{C}$  the orientation of each fibre is affected due to melting effects.

The appearance of an underlying baseline at this compaction temperature, shows that the contribution from the randomly arranged recrystallized phase is becoming more apparent.

### 3.6. Transverse strength

Transverse strengths of compacted materials, measured in bending, are shown in Fig. 14. The transverse strength rose continually with increasing compaction temperature. This is at first surprising, for once complete compaction occurs, and the fibres are "glued"

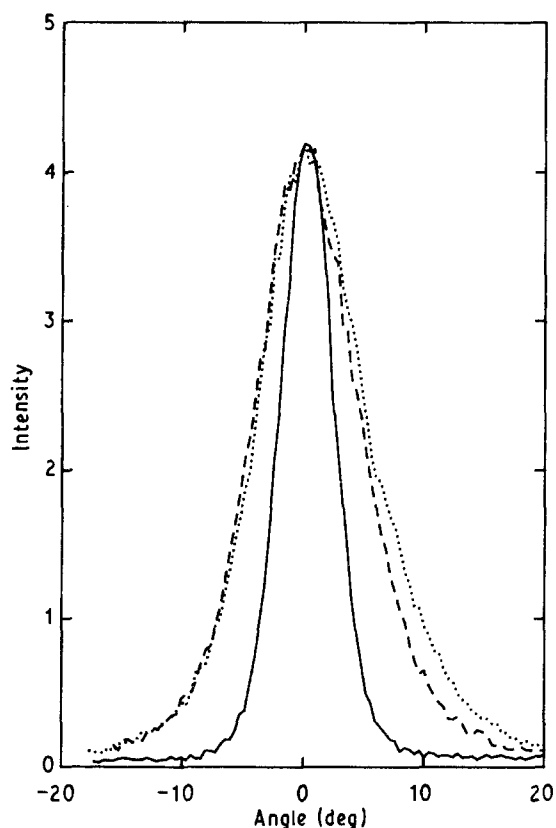


Figure 12 The 002 meridional reflection for (—) the original fibre, and for samples compacted at (---)  $136^\circ\text{C}$  and (...)  $140^\circ\text{C}$ .

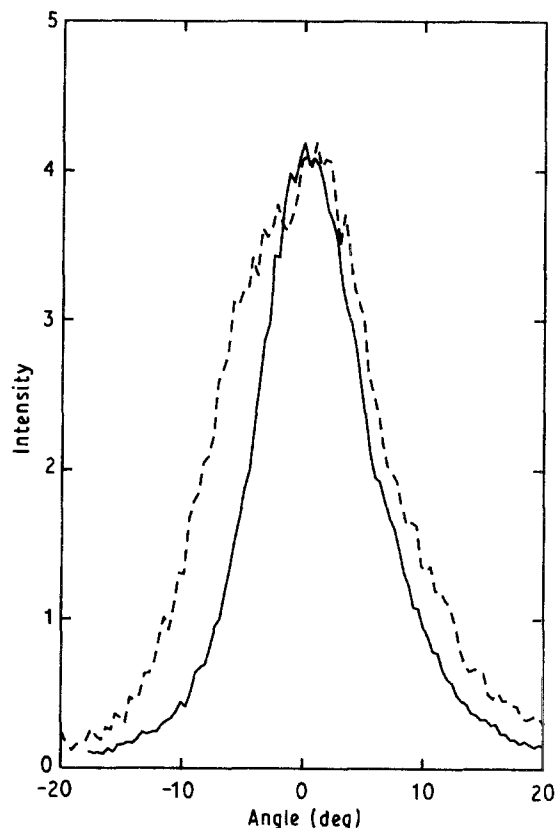


Figure 13 The 002 meridional reflection for samples compacted at (—)  $140^\circ\text{C}$  and (---)  $142^\circ\text{C}$ .

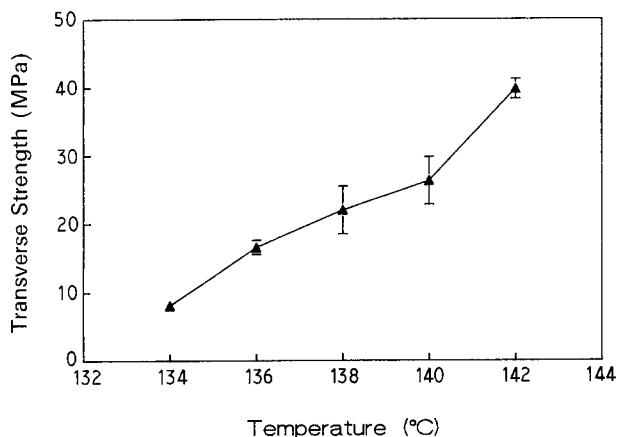


Figure 14 Transverse strength versus compaction temperature.

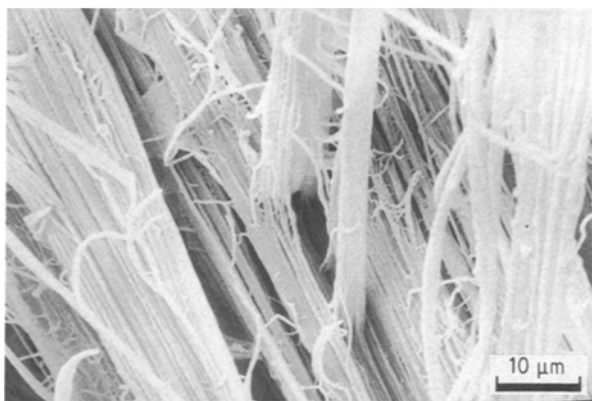


Figure 15 Transverse fracture surface showing intrafibre failure.

together, a further increase in the amount of the "second phase" might not be expected to raise the transverse strength.

The explanation of this result was obtained using scanning electron microscopy to examine a typical transverse fracture surface (Fig. 15). Knowing the typical fibre diameter to be 10 µm it is clear from the fracture surface that failure has occurred within the fibres. The presence of weak channels within each fibre has already been inferred from Fig. 5 and is considered in more detail in the following paper. Therefore once a sample is well compacted, transverse failure occurs mainly through intrafibre failure. Further increasing the compaction temperature progressively destroys the fibrillar nature of the fibre and so removes this weak mode of failure, thereby improving the transverse strength.

### 3.7. Surface modification

It has been suggested above that the primary mechanism for compaction is selective surface melting of the fibres. A way of clarifying this point is to modify the surface of the fibres and then study the effect on the compacted material. A convenient method for surface modification is plasma treatment, which has been developed in this department for treating polyethylene fibres specifically to improve the adhesion with epoxy resin [16]. The effect of the plasma treatment is to

modify the surface of the fibre both chemically and physically, including possible cross-linking [17] of the surface layer.

Bundles of Snia polyethylene fibres were given a medium plasma treatment (Power 300 W, oxygen 17 cm<sup>3</sup> min<sup>-1</sup>, speed 44 m min<sup>-1</sup>) and then compacted using the standard conditions described above at a compaction temperature of 139°C. The compacted material did not turn translucent, but remained white, and subsequent testing in the DSC showed only a very small percentage (< 1%) of the melted and recrystallized component. It can therefore be concluded that modification of the fibre surface layer by plasma treatment has inhibited surface melting making the compaction unsuccessful.

## 4. Discussion

The most fascinating aspect of the compaction process is the nature of the underlying mechanism. The etching studies (Section 3.2) clearly showed that the melted material recrystallized by nucleating on the surface of the unmelted fibre, and then grew out to fill all the gaps in the structure. However, for this growth to occur, the gaps in the structure must first be completely filled with molten polyethylene.

The unsuccessful compaction using plasma-treated fibres (Section 3.7) suggests that the majority of the initial melting occurs on the fibre surfaces. The compaction process can therefore be envisaged as follows. The fibres are placed under contact pressure at the compaction temperature for 10 min, and it is during this time that selective surface melting occurs. As shown earlier (Section 3) if the pressure is too high during this stage then selective melting is inhibited and a poor product is the result.

Following this, high pressure is applied for a short time and this squeezes the structure forcing air out and ensures that all the fibres are surrounded by molten polyethylene. On cooling, the molten material recrystallizes to bind the structure together. The mechanisms of selective surface melting are discussed further in the following paper.

The compaction process has definite parallels with the manufacture of a fibre-reinforced epoxy composite. This process always involves a high-pressure stage to squeeze the fibre and liquid resin together to expel air and compact the structure, and a final curing phase where the resin binds the structure together. One final observation which reinforces the analogy is that during compaction of the polyethylene fibres there is often flash produced on the final compacted sample which DSC examination shows to be composed of only the lower melting point phase. This can be seen to be directly analogous to squeezing out excess resin during the high-pressure compaction stage in the manufacture of a fibre-reinforced thermoset composite.

The results and observations from the previous section clearly show that the choice of compaction temperature allows a controlled portion of the virgin fibre phase to be melted, which under suitable conditions of pressure can be formed into a homogeneous

polyethylene/polyethylene composite. Fischer and Hinrichsen [18] noted similar behaviour in their work on the annealing of drawn polyethylene. They found that suitable choice of annealing temperature caused partial melting of the drawn samples which recrystallized on melting to form a second crystal population: they additionally noted that this gave rise to a double melting peak on subsequent thermal analysis. At temperatures below 138 °C, where less than 8% of the original fibre is melted, the compacted material is a three-fold composite of the original fibre, the melted and recrystallized material and entrapped air. The presence of air lowers bulk properties such as strength and density in this temperature region.

Once complete compaction is achieved, the longitudinal bulk properties pass through a maximum until the temperature is so high that a significant proportion of the original fibres are destroyed ( $> 140$  °C). In this region, above 138 °C, the compacted material is a composite of just two components, the original fibre and the melted and recrystallized material. The density and modulus of the compacted materials can be modelled using a rule of mixtures, normally used for modelling the properties of composite materials (e.g. see [12]).

The density of the compacted material,  $\rho_{\text{compacted}}$ , is simply given by

$$\rho_{\text{compacted}} = \rho_{\text{fibre}} V_f + \rho_{\text{melt}} V_m \quad (1)$$

where  $V_f$  and  $V_m$  are the volume fraction of the original and melted components, respectively. A similar relationship holds for the longitudinal modulus,  $E^L$ ,

$$E_{\text{compacted}}^L = E_{\text{fibre}}^L V_f + E_{\text{melt}} V_m \quad (2)$$

These two equations can be used to understand the changes in density and modulus seen in Figs 9 and 10. In particular, for the longitudinal modulus it is clearly seen that as the compaction temperature is increased above 138 °C, and both the longitudinal fibre modulus,  $E_{\text{fibre}}^L$ , and the proportion of fibrous material,  $V_f$ , drop; the combined effect is to cause the longitudinal modulus of the compacted material to fall rapidly. In the case of the compacted material density, this effect is not so marked because the densities of the two microstructural components differ less than their moduli.

The rule of mixtures can also be used quantitatively to predict the properties of the compacted material. For example, consider a compaction temperature of 142 °C. At this temperature, the proportions of the two phases, measured from DSC experiments, are approximately 75% melted and recrystallized and 25% original fibre. If values for the properties of the two microstructures are taken to be  $E_{\text{fibre}}^L = 42$  GPa,  $E_{\text{melt}} = 1$  GPa, then the prediction for the 142 °C compacted material is  $E_{\text{compacted}}^L = 11.3 \pm 1.5$  GPa. This value compares very well with the measured value of  $E_{\text{compacted}}^L = 10.4 \pm 0.3$  GPa.

The transverse modulus can be similarly modelled although the rule of mixtures takes on a different form

$$1/E_{\text{compacted}}^T = V_f/E_{\text{fibre}}^T + V_m/E_{\text{melt}} \quad (3)$$

Qualitatively it can be seen that changes in the various

parameters will result in a steady increase in the transverse modulus with compaction temperature.

While the longitudinal modulus and the density pass through a maximum with increasing compaction temperature, the transverse strength and modulus rise steadily throughout the range. An obvious compromise therefore exists between the different properties, allowing maximum longitudinal modulus and density to be achieved for a reasonable transverse strength. This "optimum" region is then defined as  $139 \pm 1$  °C.

The results from Section 3.6 showed that the transverse strength of the unidirectional compacted materials was governed by the transverse strength of the individual fibre. One way of improving the transverse strength of the composite would be to use a fibre with improved transverse properties. This could involve choosing a fibre of lower draw ratio, thereby sacrificing a proportion of the high longitudinal modulus.

Another possibility, which is the classic solution in composite science, is to use alternating layers of the unidirectional material to form a cross-ply laminate. A further possibility is to begin the process with sheets of woven fibre. These ideas will be reported fully in a future paper. All these processes involve a compromise between modulus and strength, and the choice of compaction route will depend on the design constraints of the final material.

## 5. Conclusions

A processing route has been discovered for the hot compaction of high-modulus melt-spun polyethylene fibres, which produces a homogeneous product and retains a high proportion of the original fibre properties while achieving a reasonable strength. This is achieved by selective surface melting of the fibres via a suitable choice of compaction temperature. On cooling, the molten material recrystallizes to form a "glue" to bind the structure together.

Hot compaction offers a route to thick-section, high-modulus polyethylene which cannot currently be produced using conventional processing techniques. The compaction process is also an easier and cheaper way of manufacturing polyethylene/polyethylene composites. The analogy with composite materials is good as the properties of the compacted materials can be understood using simple composite models.

## References

1. I. M. WARD, *Adv. Polym. Sci.* **70**, (1985) 1.
2. M. G. DOBB and J. E. McINTYRE, *ibid.* **60**, (1984) 61.
3. G. CAPACCIO and I. M. WARD, *Nature, Phys. Sci.* **243** (1973) 143.
4. P. SMITH and P. LEMSTRA, *J. Mater. Sci.* **15** (1980) 505.
5. European Pat. Appl. 83 101 731.4, filed 23 February 1983.
6. ASTM testing standards, "High Modulus Fibres and Composites" (American Society for Testing and Materials, Easton, MD, 1991).
7. R. H. OLLEY, A. M. HODGE and D. C. BASSETT, *J. Polym. Sci. Polym. Phys. Ed.* **17** (1979) 627.
8. R. H. OLLEY and D. C. BASSETT, *Polymer* **23** (1982) 1707.
9. D. C. BASSETT in "Comprehensive Polymer Sciences", Vol.1, edited by C. Booth and C. Price (Pergamon, Oxford, 1989), p. 841.
10. R. H. OLLEY, D. C. BASSETT, P. J. HINE and I. M. WARD, to be published in *J. Mater. Sci.*



11. B. WUNDERLICH, "Macromolecular Physics", Vol. 3, "Crystal Melting" (Academic Press, London, 1976).
12. D. HULL, "Composite Materials", (Cambridge University Press, Cambridge, 1981).
13. E. C. ROLLANSON, "Metallurgy for Engineers" (Edward Arnold, London, 1961).
14. D. C. BASSETT, "Principles of polymer morphology", (Cambridge University Press, Cambridge, 1981).
15. D. R. FICHTMUN and S. NEWMAN, *J. Polym. Sci. A-2* **8** (1970) 1543.
16. N. H. LADIZESKY and I. M. WARD, *Comp. Sci. Tech.* **26**, (1986) 129.
17. B. TISSINGTON, *Comp. Sci. Tech.* **44** (1992) 197.
18. E. W. FISCHER and G. HINRICHSEN, *Kolloid Z. Z. Polym.* **213** (1966) 28.

*Received 23 April  
and accepted 2 June 1992.*